Journal of Macromolecular Science, Part A
Publication details, including instructions for authors and subscription information:
http://www.informaworld.com/smpp/title~content=t713597274

Interaction of Comblike Polymethacrylates with N-Octacosane

Rocco D. Pugliese[a]; Isaac D. Rubin[a]
[a] Texaco R & D, Beacon, NY, U.S.A.

To cite this Article Pugliese, Rocco D. and Rubin, Isaac D.(1991) 'Interaction of Comblike Polymethacrylates with N-Octacosane', Journal of Macromolecular Science, Part A, 28: 1, 111 — 119

To link to this Article: DOI: 10.1080/00222339108054391

URL: http://dx.doi.org/10.1080/00222339108054391

MACROMOLECULAR REPORTS, A28(SUPPL. 2), 111-119 (1991)

INTERACTION OF COMBLIKE POLYMETHACRYLATES WITH N-OCTACOSANE

Rocco D. Pugliese and Isaac D. Rubin
Texaco R & D, Beacon, NY 12508, U.S.A.

ABSTRACT

The nature of polymethacrylate (PMA) interactions with n-octacosane (n-C_{28}) was probed using differential scanning calorimetry and powder X-ray diffraction. Blends containing comblike homopolymer and copolymer methacrylates were chosen to investigate the role of polymer side-chain crystallinity upon the crystallization behavior of n-C_{28} as a model n-paraffin compound. All PMAs disrupted the platelet morphology of the n-C_{28} while enhancing development of crystal planes along the n-paraffin chain axis. In addition, evidence supporting both orthorhombic phase stabilization and cocrystallization is reported for one solidified melt containing poly(n-octadecyl methacrylate).

INTRODUCTION

Polymethacrylates with long side chains are used extensively as pour point depressants for both lubricating oils and fuels. While such PMAs and other families of pour depressant additives have been used commercially for many years, their mechanisms of interaction in the wax crystallization process are still not clearly understood.[1-4]

It is now generally accepted that pour point depressants work either by adsorption onto the nascent n-paraffin crystals or by their ability to cocrystallize with the n-paraffins so both are incorporated within the same crystal lattice. In either case, the net effect as the oil is cooled is a weaker wax network which in turn lowers the temperature at which the wax congeals the oil. Our main thrust in this area is to find better means to identify the action mechanisms of PMAs as a guide to the development of superior pour point depressants.

Because of the difficulties in measuring and interpreting crystallization phenomena in lubricating oils, we have focused our studies on simple model systems without diluent base oil. This article thus examines the effect of comblike homopolymer and copolymer methacrylates upon n-C_{28} crystallized from melts. They represent a range of materials differing in side-chain structure and crystallinity. Our approach provides information on macro- and microstructure including average crystal morphology, phase transformation, and lattice modification. It also provides a foundation for exploring the more complex behaviors of oil solution crystallization. The characterization tools used were differential scanning calorimetry (DSC) and powder X-ray diffraction (XRD).

EXPERIMENTAL

All polymethacrylates were made by free-radical polymerization in cyclohexane at reflux using azobisisobutyronitrile as the catalyst. They were precipitated into methanol and then washed several times with hot methanol and acetone and dried to constant weight under vacuum at temperatures below 70^0C. Reaction products were analyzed for side-chain carbon number distribution by pyrolysis gas chromatography. Weight average (M_w) and number average (M_n) molecular weights were obtained by gel permeation chromatography and ranged from 150,000 - 240,000 for M_w and from 75,000 - 120,000 for M_n. Heats of melting (ΔH_m) and melting temperatures (T_m) were obtained by DSC. PMA compositional data are given in Table 1 while ΔH_m and T_m values are included in Table 2. The n-C_{28} was 97% pure material purchased from Alfa Products, Morton Thiokol, Inc. and was used without further purification.

Blends were prepared by mixing n-C_{28} and polymer in a 5:1 weight ratio, heating the mixtures to 85^0C with occasional stirring until they were completely uniform in appearance. The melts were allowed to air-cool to room temperature and samples of crystallized products were examined by DSC and powder XRD. Samples of neat components were similarly analyzed.

DSC runs were obtained on 10-25 mg samples using a Perkin-Elmer DSC-7 at a heating rate of 10 ^0C/min. Heats of melting, obtained from areas under the curves, were repeatable within 15%. Melting temperatures were determined from the endotherm maximum of the melting transition.

Powder XRD data were obtained using a Scintag PAD V diffractometer with Cu K-alpha radiation, graphite monochromator, and a scintillation detector. Diffraction scans were run from 2 to 40^0 two-theta at a rate of 2

TABLE 1

GC Analysis of Comblike Polymethacrylates

R Group Distr.(wt%)	H-16	H-18	C-13	C-14
C_4	-	-	-	15
C_{10}	-	-	2	-
C_{12}	-	-	51	7
C_{13}	0.7	-	2	8
C_{14}	0.5	-	27	13
C_{15}	0.8	-	2	10
C_{16}	97.8	-	10	22
C_{18}	0.2	98	6	16
C_{20}	-	-	-	8
C_{22}	-	-	-	0.5

H-XX, C-XX designate homopolymer and copolymer, respectively; XX is the average carbon number of the ester R group.

TABLE 2

ΔH_m and T_m for n-C_{28} and PMA Components in Their 5:1 Mixtures

PMA in	ΔH_m, J/g			T_m, ^{0}C		
Mixture	n-C_{28}[a,b]	PMA	PMA^0	n-C_{28}	PMA	PMA^0
H-16	274	26	33	65	17	19
H-18	145	164	59	61	36	31
C-13	263	<5	7	64	-30	-30
C-14	275	7	16	64	-1	-5

---

[a] ΔH_m for n-C_{28} melting includes solid-solid and melting transformations.

[b] For neat n-C_{28}, ΔH_m = 269 J/g (doublet) and T_m = 64^{0}C. PMA refers to PMA components in mixture; PMA^0 refers to the neat components.

^{0}/min in steps of 0.03^{0}; beam collimation was achieved using a 2^{0} divergence slit and a 0.3 mm receiving slit. Powder specimens for analysis were obtained by grinding the samples in a mortar and pestle at dry ice temperature, warming the pulverized solid to room temperature, and sieving through a 100 mesh (150 micron opening) screen. The sieved powders were transferred to quartz plate zero-background sample supports by dispersing about 5 mg of 100 mesh powder onto the support surface, which was recessed 100 micrometers from the diffractometer focusing plane surface. D-spacing measurements for these preparations were repeatable within 0.04 and 0.003 Å for (002) and (110) n-octacosane reflections, respectively. Early work using standard packed powder mounts was abandoned due to severe losses in resolution caused by low mass absorption of the hydrocarbon samples[5] and from preferred orientation complications arising from the platelet morphology of the n-C_{28}.

RESULTS AND DISCUSSION

The pertinent thermal properties obtained from the DSC scans of the four PMAs and their mixtures with n-C_{28} are summarized in Table 2. Overall, the melting behavior of the mixtures with PMAs H-16, C-13, and C-14 is very similar. There are no significant changes in the n-C_{28} endotherm with repect to its heat or temperature of melting while the PMA endotherm reflects a trend of lower heats and temperatures of melting than those of the original PMAs. Stated differently, the lattices of H-16, C-13, and C-14 comblike PMAs are modified to some degree by the n-C_{28}, but its lattice is not disturbed, allowing independent n-C_{28} crystallization from the melt mixtures. In contrast, the H-18 PMA dramatically changes both the n-C_{28} and H-18 original endotherm behavior as shown in Table 2 and Figure 1. With respect to qualitative peak shape effects, the well-resolved doublet for the n-C_{28} solid-solid and solid-liquid transformations become diffused as a broad band with several inflections shifted towards lower melting temperatures. In just the opposite direction, the broad H-18 peak becomes sharpened and its melting temperature increases about 5 ^{0}C. These observations and ΔH_m values that are one-half that expected for n-C_{28}, decreasing from 269 to 145 J/g, and two and one-half times that expected for H-18, rising from 59 to 164 J/g, provide evidence of appreciable component interaction. Since lattice modification of both components appears to be involved - crystallinity increasing for the H-18 while decreasing for n-C_{28} - it seems reasonable they are, at least partially, end-members of a solid solution series. Such

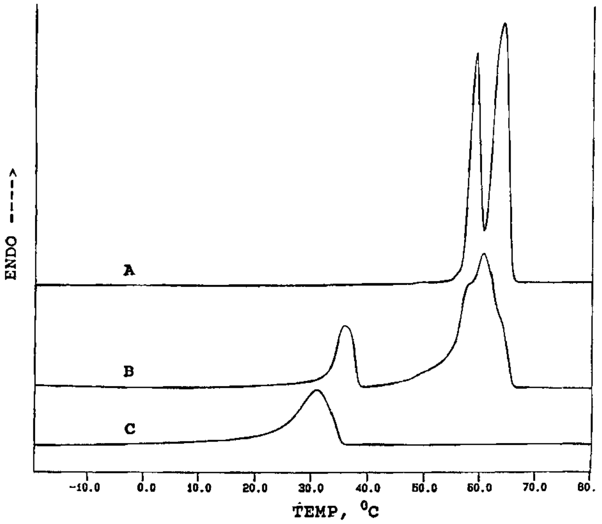

FIG. 1. DSC melting curves of (A) n-C_{28}; (B) 5:1 n-C_{28}/H-18; (C) H-18 PMA.

cocrystallization, was previously observed by us with blends of n-dodecane and H-18.[6]

Powder XRD results obtained on the neat n-C_{28} gave a long spacing of 33.4 Å and short spacings of 3.74, 4.07, 4.25 and 4.38 Å, consistent with the β_m monoclinic crystal structure.[7] In accordance with Broadhurst's nomenclature system,[8] the n-paraffin monoclinic phase is termed β_m, while the orthorhombic phase is termed β_o. As can be seen in the XRD scans in Figure 2, the β_m lattice is preserved for the most part upon crystallization from melts containing different PMAs. All the discrete diffraction peaks are ascribed to the n-C_{28} phase(s), and compared to the n-paraffin, even the most crystalline PMA (H-18) contributes only weak, diffuse bands slightly above background intensity.

D-spacing values (Table 3) for the β_m phase (001) and (110) peaks are invariant for all the solidified melts indicating the PMAs do not modify the original n-C_{28} unit cell dimensions. Although there is no evidence of isostructural modification from the diffraction parameters in Table 3, there is indeed polymorphic change which is discussed further below. In terms of isostructural modification of the PMA lattices in the solidified melts, this cannot be determined from the

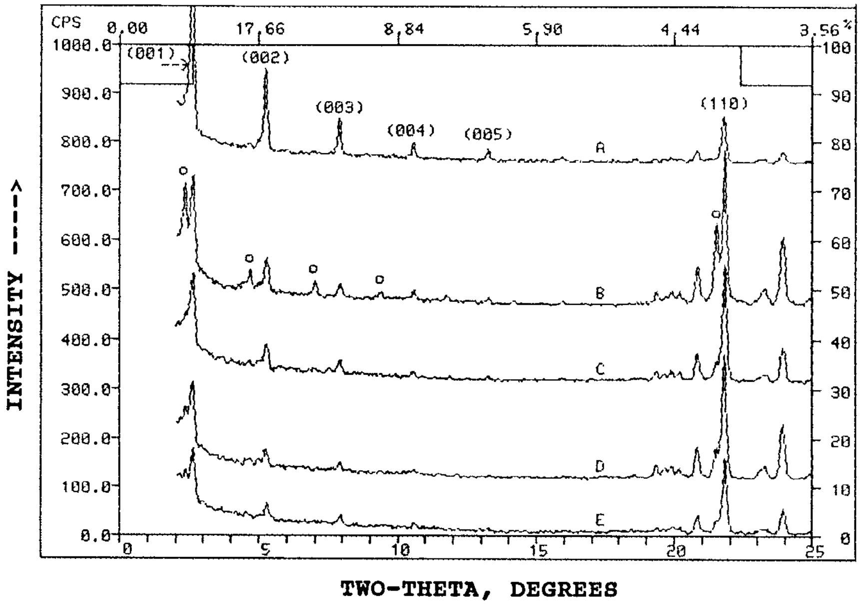

FIG. 2. XRD powder patterns of (A) β_m n-C_{28} phase and (B-E) 5:1 n-C_{28}/PMA solidified melts containing: (B) H-18; (C) H-16; (D) C-14; (E) C-13. Peaks marked "o" denote β_o n-C_{28} phase.

diffraction data but DSC measurements previously discussed can be used to help address such interactions.

Mean crystallite shapes of the paraffin aggregates can be qualitatively assessed from the relative intensities of (00l) and (hk0) peaks in the powder pattern and by preferential broadening of the (00l) peak. The scans in Figure 2 show quite clearly a sharp decrease of (00l) and an increase of (110) intensities for all crystallized melts containing PMAs. This is interpreted as a morphology change from the original plate-like n-C_{28} to needle-like crystalline aggregates. Thus, the PMA interferes with the n-paraffin growth and development of lamellar planes intersecting the chain axis while it enhances growth in the plane parallel to it. The preferential broadening of the (002) and no shifting or broadening of the (110) planes (Table 3) are attributed solely to crystal quality or habit changes as opposed to structural changes on a molecular (unit cell) level.

TABLE 3

X-ray Parameters
Effect of PMAs on β_m n-C_{28} Lattice

PMA in Mixture	d (Å) (001)[a]	d (Å) (110)	FWHM[1] (002)	FWHM[1] (110)
None	33.4	4.073	.094	.146
H-16	33.3	4.067	.116	.151
H-18	33.3	4.068	.125	.142
C-13	33.4	4.072	.110	.141
C-14	33.4	4.070	.124	.156

---

[1] Peak full-width at half-maximum, °2θ.
[a] Calculated from higher order reflections.

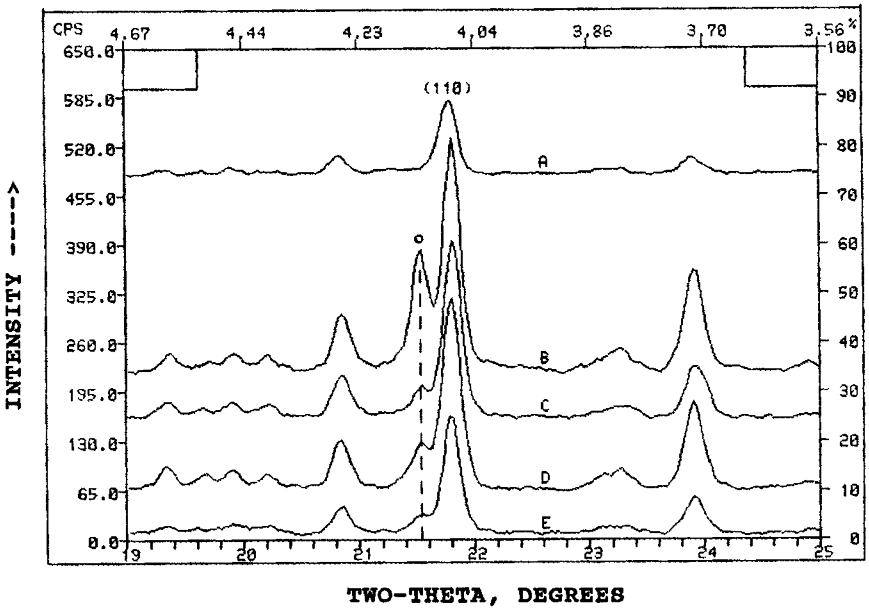

FIG. 3. (hk0) diffraction region showing splitting for n-C_{28} β_m ---> β_o transition. Curve designations as in Fig. 2.

TABLE 4

Assignment of New Peaks Found in the n-C_{28}/PMA Solidified Melt

(hkl)	2θ (°)	d (Å)
(001)	-	37.5[a]
(002)	7.054	12.52
(003)	9.422	9.380
(110)	21.551	4.120

---

[a] Calculated from (002) and (003) peaks.

Additional peaks (Figure 2, curve B) which are observed on the low angle side of β_m n-C_{28} peaks point to the formation of a second crystalline phase. Closer inspection of the (hk0) region (Figure 3) shows weak splitting of the (110) peak for mixtures containing PMAs H-16, C-13 and C-14, strong splitting for H-18, and no splitting in the neat n-C28. D-spacings and peak assignments for the additional peaks in Figure 2B are shown in Table 4. The observed long spacing of 37.5 Å agrees closely with the published value of 37.7 Å for the β_o n-C_{28} polymorph.[8] From relative diffraction intensities the amount of β_o form is about one-half that of the β_m, indicating the formation of a eutectic mixture in the solidified melt containing H-18 PMA. The mixtures with other PMAs, on the other hand, exhibit only slight tendency toward stabilization of the β_o form (Figure 3) and the formation of eutectics.

In conclusion, compared to other homopolymer and copolymer methacrylates investigated, poly(n-octadecyl methacrylate) interacts more extensively with n-octacosane in stabilizing its high temperature β_o form to yield a eutectic composition of n-C_{28} polymorphs. Since the β_o structure is also common to poly(n-octadecyl methacrylate),[9] both components could cocrystallize in this lattice, while for the other PMAs this basic structural requirement for cocrystallization is not satisfied. DSC results are consistent with coexisting β_m and β_o n-C_{28} forms and the incorporation of the β_o n-C_{28} into the poly(n-octadecyl methacrylate) lattice.

REFERENCES

(1) E. F. Jordan, Jr., S. Smith, Jr., R. D. Zabarsky, A. N. Wrigley, J. Appl. Polym. Sci. **22** (1978) 1547.

(2) M. Chichakli and F. W. Jessen, Ind. Eng. Chem. **59** (1967) 86.

(3) G. A. Holder and J. Winkler, J. Inst. Pet. **51** (1965) 235.

(4) L.E. Lorensen, ACS Meeting (Sept. 1962) B-61.

(5) D. T. Keating and B. E. Warren, Rev. Sci. Instr. **23** (1952) 519.

(6) I. D. Rubin and R. D. Pugliese, Angew. Makromol. Chem. **171** (1989) 165.

(7) J. D. Hoffman and B. F. Decker, J. Phys. Chem. **57** (1953) 520.

(8) M. G. Broadhurst, J. Res. Natl. Bur. Stand. **66A** (1962) 241.

(9) K. Yokota, T. Kougo and T. Hirabayashi, Polym. J. (Tokyo) **15** (1983) 891.